

Research Article

Anticancer Efficacy of a Difluorodiarylidene Piperidone (HO-3867) in Human Ovarian Cancer Cells and Tumor Xenografts

Karuppaiyah Selvendiran¹, Liyue Tong¹, Anna Bratasz¹, M. Lakshmi Kuppasamy¹, Shabnam Ahmed¹, Yazhini Ravi¹, Nancy J. Trigg¹, Brian K. Rivera¹, Tamás Kálai³, Kálmán Hideg³, and Periannan Kuppasamy^{1,2}

Abstract

The purpose of this study was to evaluate the anticancer potency and mechanism of a novel difluorodiarylidene piperidone (H-4073) and its N-hydroxypyrroline modification (HO-3867) in human ovarian cancer. Studies were done using established human ovarian cancer cell lines (A2870, A2780cDDP, OV-4, SKOV3, PA-1, and OVCAR3) as well as in a murine xenograft tumor (A2780) model. Both compounds were comparably and significantly cytotoxic to A2780 cells. However, HO-3867 showed a preferential toxicity toward ovarian cancer cells while sparing healthy cells. HO-3867 induced G₂-M cell cycle arrest in A2780 cells by modulating cell cycle regulatory molecules p53, p21, p27, cyclin-dependent kinase 2, and cyclin, and promoted apoptosis by caspase-8 and caspase-3 activation. It also caused an increase in the expression of functional Fas/CD95 and decreases in signal transducers and activators of transcription 3 (STAT3; Tyr705) and JAK1 phosphorylation. There was a significant reduction in STAT3 downstream target protein levels including Bcl-xL, Bcl-2, survivin, and vascular endothelial growth factor, suggesting that HO-3867 exposure disrupted the JAK/STAT3 signaling pathway. In addition, HO-3867 significantly inhibited the growth of the ovarian xenografted tumors in a dosage-dependent manner without any apparent toxicity. Western blot analysis of the xenograft tumor tissues showed that HO-3867 inhibited pSTAT3 (Tyr705 and Ser727) and JAK1 and increased apoptotic markers cleaved caspase-3 and poly ADP ribose polymerase. HO-3867 exhibited significant cytotoxicity toward ovarian cancer cells by inhibition of the JAK/STAT3 signaling pathway. The study suggested that HO-3867 may be useful as a safe and effective anticancer agent for ovarian cancer therapy. *Mol Cancer Ther*; 9(5); 1169–79. ©2010 AACR.

Introduction

Ovarian cancer is the second most commonly diagnosed gynecologic malignancy among women in the United States (1, 2). The current standard of care includes primary surgical cytoreduction followed by administration of cisplatin or carboplatin in combination with taxanes (3). Long-term administration of cisplatin has been shown to result in the development of chemotherapeutic drug resistance in the cancer cell population (4, 5). An increase in the cisplatin resistance of ovarian tumors requires the administration of larger doses of the drug that may lead to debilitating side effects, including severe

multiorgan toxicities (6). Many chemotherapeutic drugs induce the production of reactive oxygen species, which are toxic to both cancerous and healthy cells. To reduce the side effects of chemotherapy and improve the quality of life, the majority of cancer patients use antioxidants in combination with conventional therapies. Unfortunately, adding antioxidants adjunctively may compromise the efficacy of these conventional therapeutic strategies (7).

Signal transducer and activator of transcription 3 (STAT3) has been implicated in the pathogenesis of a variety of human malignancies including head and neck cancer, myeloma, prostate cancer, breast cancer, colon cancer, and ovarian cancer (8–11). Activation of STAT3 can be accomplished by the Janus kinases (JAK; including TYK2), activated epidermal growth factor receptor, and Src kinase (12). STAT3 is constitutively activated in many tumor types and this activation promotes acceleration of cell proliferation, upregulation of survival factors, and activation of antiapoptotic proteins. This imparts cellular resistance to chemotherapy by inhibiting apoptosis in epithelial malignancies, including ovarian cancer (13, 14). Because of its important role in oncogenesis, STAT3 has attracted much attention as a potential pharmacologic target for cancer treatment (11, 15, 16).

Authors' Affiliations: ¹Department of Internal Medicine, Davis Heart and Lung Research Institute and ²Comprehensive Cancer Center, The Ohio State University, Columbus, Ohio; and ³Institute of Organic and Medicinal Chemistry, University of Pecs, Pecs, Hungary

Note: K. Selvendiran and L. Tong contributed equally to this work.

Corresponding Author: Periannan Kuppasamy, The Ohio State University, 420 West 12th Avenue, Room 114, Columbus, OH 43210. Phone: 614-292-8998; Fax: 614-292-8454. E-mail: kuppasamy.1@osu.edu

doi: 10.1158/1535-7163.MCT-09-1207

©2010 American Association for Cancer Research.

Curcumin, a β -diketone constituent of turmeric derived from the rhizome of the plant *Curcuma longa*, has been shown to inhibit the many cellular signaling pathways, including the JAK-STAT pathway, and to down-regulate the expression of many tumor-promoting downstream proteins and signaling cascades (16, 17). Curcumin has been shown to have antiproliferative and antiangiogenic activities in several tumors, including ovarian cancer (18, 19). However, the clinical use of curcumin has been limited due to its low anticancer activity and poor absorption. Recently, a novel class of curcumin analogues, diarylidenyl piperidones (DAP), has been developed by incorporating a piperidone link to the β -diketone structure and fluorosubstitutions on the phenyl groups (20). The DAP compounds, in general, were more

effective than curcumin in inhibiting the proliferation of a variety of cancer cell lines (21). EF24, one of the DAP compounds with *ortho*-fluorinated phenyl groups, exhibited potent anticancer efficacy *in vitro* when tested using breast cancer (21), colon cancer (22), and ovarian epithelial cancer (23) cell lines. Subsequently, we observed that H-4073 (Fig. 1), a *para*-fluorinated variant, was more potent than EF24 in inducing cytotoxicity to ovarian cancer cells (24, 25).

A nonspecific cytotoxic compound may have side effects caused by damage to normal cells. For example, many chemotherapeutic agents act by producing free radicals, which may increase oxidative stress in normal cells (26, 27). To minimize this toxicity, there is a need to use detoxicants, such as antioxidants, which can differentiate

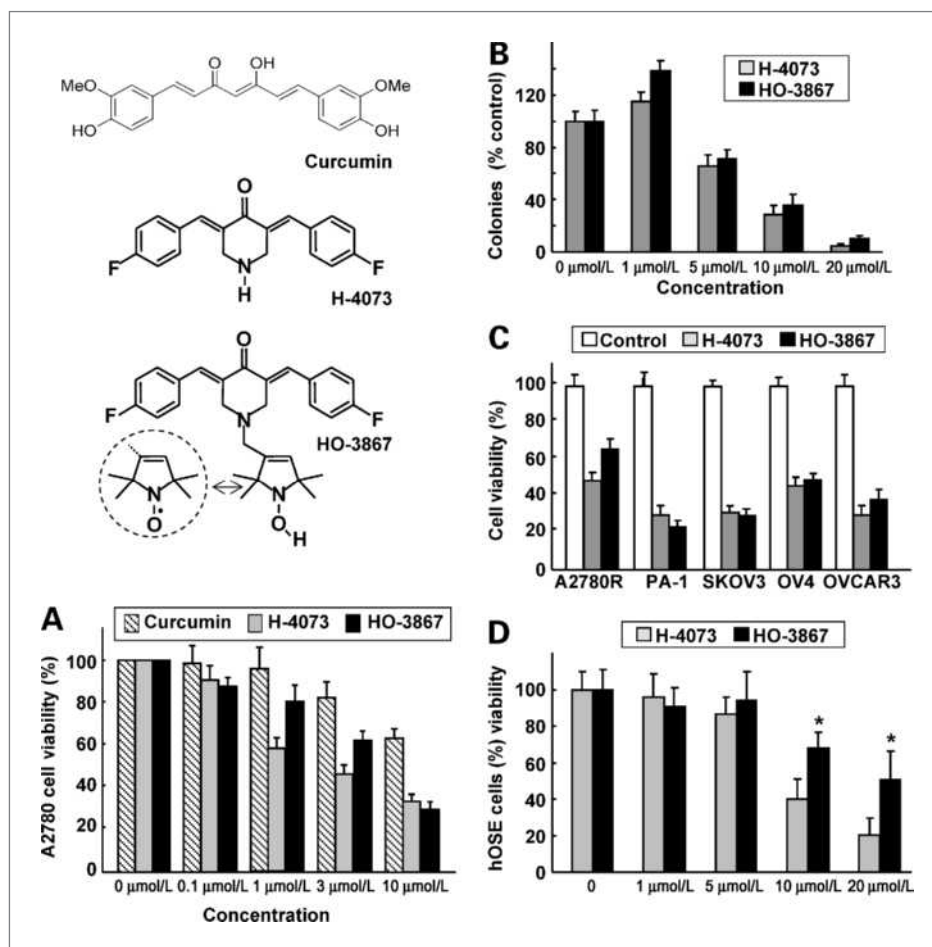


Figure 1. Inhibition of cell viability and proliferation by HO-3867. Structures of curcumin, H-4073, and HO-3867 are shown. H-4073 is a 3,5-diarylidenyl piperidone containing a *para*-fluorosubstitution on the phenyl groups. HO-3867 contains an N-hydroxy-pyrroline moiety covalently linked to the NH_2 -terminus of piperidone. In aerated solutions and cells, the N-hydroxy-pyrroline undergoes conversion to and exists in equilibrium with the nitroxide ($>\text{NO}$) form (shown in the circle). A, dose-dependent effect of curcumin, H-4073, and HO-3867 on the viability of A2780 cells. Cells were incubated with curcumin, H-4073, or HO-3867 for 24 hours followed by measurement of cell viability (by MTT assay). Columns, mean ($n = 5$); bars, SEM. B, dose-dependent effect of H-4073 and HO-3867 on the colony-forming ability of A2780 cells. Columns, mean ($n = 5$); bars, SEM. C, effect of H-4073 and HO-3867 (10 $\mu\text{mol/L}$; 24 h) on the viability of different ovarian cancer cell lines: A2780R (cisplatin-resistant variation of A2780), SKOV3, OV3, and OVCAR3. Columns, mean ($n = 5$); bars, SEM. D, dose- and incubation time-dependent effect of HO-3867 (10 $\mu\text{mol/L}$) on the viability of hOSE, a human ovary surface epithelial cell line used as a healthy control. Columns, mean ($n = 5$); bars, SEM. *, $P < 0.05$ versus the effect of H-4073 at equivalent doses.

between healthy and cancerous cells and selectively protect the healthy cells by scavenging free radicals (28, 29). It has been shown that nitroxides, a class of small-molecular-weight heterocyclic molecules containing " $>NO$," and hydroxylamines, the one electron-reduced form of nitroxides characterized by " $>NOH$," preferentially scavenge oxygen radicals in cells that have normal oxygenation or redox status (30, 31). Hydroxylamines are called "pro-nitroxides," as the hydroxylamine form of the molecules exists in equilibrium with the nitroxide form in well-oxygenated tissues (30, 31). Most tumors are hypoxic in nature and their cellular environment is more reducing (for example, thiol rich) when compared with healthy cells (32, 33). This differential aspect between normal and cancerous cells has led us to the design of HO-3867 (Fig. 1), which would have both anticancer and antioxidant properties (25). Hence, the specific goals of the present study were (a) to determine the anticancer efficacy of HO-3867 toward cancerous and a noncancerous (control) cell lines, (b) to derive mechanistic insights into the action of HO-3867, and (c) determine whether HO-3867 would significantly inhibit tumor growth in an *in vivo* model of ovarian cancer. The studies were conducted using human ovarian cancer cell lines and a murine xenograft model of ovarian cancer. The results showed a preferential toxicity of HO-3867 toward ovarian cancer cells and suppression of tumor growth through inhibition of the JAK/STAT3 pathway both *in vitro* and *in vivo*.

Materials and Methods

Chemicals

Curcumin, superoxide dismutase, 6-carboxy-2',7'-dichlorodihydrofluorescein diacetate, diacetoxy-methyl ester, MTT, and antibodies against actin were obtained from Sigma. 5-Diethoxyphosphoryl-5-methyl-1-pyrroline-*N*-oxide was from Radical Vision. Cell-culture medium (RPMI 1640), fetal bovine serum, antibiotics, sodium pyruvate, trypsin, and PBS were purchased from Life Technologies. Polyvinylidene fluoride membrane and molecular weight markers were obtained from Bio-Rad. Antibodies against poly-adenosine diphosphate ribose polymerase (PARP), cleaved caspase-3, caspase-7, caspase-8, STAT3, phospho-STAT3 (Tyr705), JAK1, Bcl-xL, and phospho-JAK1 (Tyr1022/1023) were purchased from Cell Signaling Technology. Antibodies specific for cyclin A, cyclin D1, cyclin-dependent kinase (Cdk)2, p53, p21, p27, Fas/CD95, FasL, Bcl-2, and ubiquitin were purchased from Santa Cruz Biotechnology. Enhanced chemiluminescence reagents were obtained from Amersham Pharmacia Biotech (GE Healthcare). All other reagents, of analytical grade or higher, were purchased from Sigma-Aldrich unless otherwise noted.

Synthesis of H-4073 and HO-3867

Melting points were determined with a Boetius micro-melting point apparatus and are uncorrected. Elemental analyses (C, H, N, S) were done on a Fisons EA 1110

CHNS elemental analyzer. Mass spectra were recorded on Thermoquest Automass Multi and VG TRIO-2 instruments the EI mode. 1H NMR spectra were recorded with a Varian UNITYINOVA 400 WB spectrometer. Chemical shifts are referenced to Me_4Si . Measurements were run at 298K probe temperature in a $CDCl_3$ solution. Flash column chromatography was done on a Merck Kieselgel 60 (0.040–0.063 mm). Qualitative thin-layer chromatography was carried out on commercially prepared plates (20 × 20 × 0.02 cm) coated with Merck Kieselgel GF₂₅₄. All chemicals were purchased from Aldrich. Compound HO-350 was prepared as described earlier (34).

(3E,5E)-3,5-Bis(4-fluorobenzylidene)piperidin-4-one (H-4073). A solution of 4-fluorobenzaldehyde (2.48 g, 20.0 mmol) and 4-piperidone hydrate hydrochloride (1.53 g, 10.0 mmol) was allowed to stay in glacial acetic acid (saturated with HCl gas previously) for 2 days. The precipitated yellow solid was filtered, washed with Et_2O (30 mL), and the yellow hydrochloride salt 2.50 g (72%; melting point, 212–214°C) was air dried and used in the next step without further purification. For analytic characterization, 300 mg of the salt were dissolved in water (10 mL) and basified by addition of 250 mg K_2CO_3 and extracted with $CHCl_3$ (3 × 10 mL). The combined extracts were dried ($MgSO_4$), filtered, and evaporated to obtain a yellow solid compound [R_f : 0.43 ($CHCl_3/Et_2O$, 2:1). MS (EI, 70 eV): m/z (%): 311 (M^+ , 73) 282 (43), 148 (36), 133(100). Anal Calcd. for: $C_{19}H_{15}F_2NO$: C 73.30; H 4.86; N 4.50. Found: C 73.19; H 4.83; N 4.32. 1H NMR (399.9 MHz, $DMSO-d_6$): δ 4.38 (s, 4 H), 7.26 (t, 4 H), 7.48 (m, 4H), 7.81 (s, 2H)].

1-[(1-Oxyl-2,2,5,5-tetramethyl-2,5-dihydro-1H-pyrrol-3-yl)methyl]-(3E,5E)-3,5-Bis(4-fluorobenzylidene)piperidin-4-one (HO-3867). A mixture of H-4073 HCl salt (1.73 g, 5.0 mmol) and K_2CO_3 (1.38 g, 10.0 mmol) in acetonitrile (20 mL) was stirred at room temperature for 30 minutes. Then, allylic bromide and HO-350 (1.28 g, 5.5 mmol) were added dissolved in acetonitrile (5 mL) and the mixture was stirred and refluxed till the consumption of the starting materials (~3 h). After cooling, the inorganic salts were filtered off on sintered glass filter, washed with $CHCl_3$ (10 mL), the filtrate was evaporated, and the residue was partitioned between $CHCl_3$ (20 mL) and water (10 mL). The organic phase was separated; the aqueous phase was washed with $CHCl_3$ (20 mL); and the combined organic phase was dried ($MgSO_4$), filtered, and evaporated. The residue was purified by flash column chromatography (Hexane/ $EtOAc$) to obtain the deep yellow solid title compound [1.36 g (59%), R_f : 0.57 (Hexane/ $EtOAc$, 2:1), mp 142–144°C. MS (EI, 70 eV): m/z (%): 463 (M^+ , 12) 433 (20), 324 (40), 310 (43), 133(100). Electron spin resonance: $a_N = 14.9$ G. Anal Calcd. for: $C_{28}H_{29}F_2N_2O_2$: C 72.55; H 6.31; N 6.04. Found: C 72.54; H 6.23; N 6.04].

To achieve the *N*-hydroxy compound HCl salt, HO-3867 (1.0 g) was dissolved in ethanol (20 mL, saturated with HCl gas previously) and refluxed for 30 minutes. Then, the solvent was evaporated off and the procedure was

repeated till the disappearance of the electron paramagnetic resonance triplet line to give the HCl salt.

A detailed report on the synthesis and structure-activity relationship of a number of DAP derivatives will be published separately (35). Stock solutions of the compounds were freshly prepared in DMSO.

Cell lines and cultures

The A2780 human epithelial ovarian cancer cell line was used for most parts of the study. Other ovarian cancer cell lines used (SKOV3, OVCAR3, A2780R, and OV4), as were normal human ovarian surface epithelial (hOSE; ScienCell Ovarian Cell System) cells, were grown in RPMI 1640 and DMEM supplemented with 10% fetal bovine serum, 2% sodium pyruvate, 1% penicillin, and 1% streptomycin. Cells were grown in a 75-mm flask to 70% confluence at 37°C in an atmosphere of 5% CO₂ and 95% air. Cells were routinely trypsinized (0.05% trypsin/EDTA) and counted using an automated counter (NucleoCounter, New Brunswick Scientific).

Cell viability by MTT assay

Cell viability was determined by a colorimetric assay using MTT. In the mitochondria of living cells, yellow MTT undergoes a reductive conversion to formazan, producing a purple color. Cells, grown to ~80% confluence in 75-mm flasks, were trypsinized, counted, seeded in 96-well plates with an average population of 7,000 cells per well, incubated overnight, and then treated with curcumin, H-4073, or HO-3867 for 24 hours. All experiments were done using eight replicates and repeated at least thrice.

Cell proliferation by clonogenic assay

Cell survival was assessed by clonogenic assay. Cells at ~80% confluence were trypsinized, rinsed, seeded onto 60-mm dishes (5×10^4 cells per dish), grown for 24 hours at 37°C, and treated afterward with H-4073 or HO-3867 for 24 hours. Nontreated cells served as controls. After treatment, the cells were washed twice with PBS, trypsinized, counted, and plated in 60-mm dishes in triplicate and incubated for an additional 7 days. The colonies were then stained with crystal violet (in ethyl alcohol) and counted using an automated colony counter (ColCount, Oxford Optronix). Each experiment was repeated at least five times.

Cell-cycle analysis

Cells were treated with HO-3867 (10 μ mol/L) for 24 hours, trypsinized, washed in PBS, and fixed in an ice-cold 75% ethanol/PBS solution. The DNA was labeled with propidium iodide. Cells were sorted by flow cytometry and cell cycle profiles were determined using ModFit LT software (Becton Dickinson).

Immunoblot analysis

Cells in RPMI 1640 were treated with DMSO (control) or HO-3867 (10 μ mol/L) for 24 hours. Equal volumes of DMSO (0.1% v/v) were present in each treatment. Fol-

lowing treatment, the cell lysates were prepared in non-denaturing lysis buffer containing 10 mmol/L Tris-HCl (pH 7.4), 150 mmol/L NaCl, 1% Triton X-100, 1 mmol/L EDTA, 1 mmol/L EGTA, 0.3 mmol/L phenylmethylsulfonyl fluoride, 0.2 mmol/L sodium orthovanadate, 0.5% NP40, 1 μ g/mL aprotinin, and 1 μ g/mL leupeptin. The lysates were centrifuged at $10,000 \times g$ for 20 minutes at 4°C and the supernatant was separated. The protein concentration in the lysates was determined using a Pierce detergent-compatible protein assay kit. For Western blotting, 25 to 50 μ g of protein lysate per sample were denatured in 2 \times SDS-PAGE sample buffer and subjected to SDS-PAGE on a 10% tris-glycine gel. The separated proteins were transferred to a polyvinylidene fluoride membrane and were blocked with 5% nonfat milk powder (w/v) in TBST (10 mmol/L Tris, 10 mmol/L NaCl, 0.1% Tween 20) for 1 hour at room temperature or overnight at 4°C. The membranes were then incubated with the primary antibodies. The bound antibodies were detected with horseradish peroxidase-labeled sheep anti-mouse IgG or horseradish peroxidase-labeled donkey anti-rabbit IgG using an enhanced chemiluminescence detection system (ECL Advanced kit). Protein expressions were determined using the Image Gauge v. 3.45 software.

Ovarian cancer tumor xenografts in mice

Cultured A2780 cancer cells (2×10^6 cells in 60 μ L of PBS) were s.c. injected into the back of 6-week-old BALB/c nude mice from the National Cancer Institute. Five to 7 days later, when the tumors reached 3 to 5 mm in diameter, the mice were divided ($n = 9$ /group) in a manner to equalize the mean tumor diameter among the groups. The control group was given a normal diet (no treatment), whereas the experimental groups were treated using the DAP compounds mixed with the animal feed (Harlan Teklad) at three different levels (25, 50, and 100 ppm). The doses were chosen based on an initial dose-response study optimized to produce an observable effect on tumor growth. The size of the tumor was measured twice per week using a digital Vernier caliper. The tumor volume was determined from the orthogonal dimensions (d_1, d_2, d_3) using the formula $(d_1 \times d_2 \times d_3) \times \pi/6$. Thirty five days after the beginning of HO-3867 treatment, the mice were sacrificed and the tumors were resected. The tumor tissues were then subjected to immunoblot analysis.

Data analysis

The statistical significance of the results was evaluated using ANOVA and a Student's *t* test. A *P* value of <0.05 was considered significant.

Results

HO-3867 is cytotoxic to A2780 and other ovarian cancer cell lines

The cytotoxic effects of H-4073 and HO-3867 were evaluated and compared with that of curcumin in A2780 and other established human ovarian cancer cell

lines. Fig. 1A compares the effect of curcumin, H-4073, and HO-3867 on the viability of A2780 cells. Although all three compounds showed a dose-dependent cytotoxicity, H-4073 and HO-3867 exhibited significantly higher toxicity when compared with curcumin. The results further indicated that the cytotoxic effects of HO-3867 and H-4073 on A2780 cells were comparable, suggesting that the introduction of the N-hydroxypyrroline moiety in HO-3867 did not compromise the cytotoxic effect of HO-3867 against A2780 cells. We next did clonogenic assays to study the effectiveness of H-4073 and HO-3867 on the proliferation of A2780 cells. Both compounds showed a dose-dependent reduction in the number of colonies (Fig. 1B), suggesting that the compounds are equally potent in inhibiting cell proliferation. We further tested the cytotoxicity of H-4073 and HO-3867 in a number of other well-established human ovarian cancer cell lines including a cisplatin-resistant derivative of A2780 (A2780R), PA-1, SKOV3, OV4, and OVCAR3. The results (Fig. 1C) showed that both H-4073 and HO-3867 were equally and significantly toxic to the tested cell lines. We then tested the effect of HO-3867 exposure on hOSE cells, which are noncancerous control cell lines derived from human ovarian surface epithelium. As shown in Fig. 1D, no significant cytotoxicity to hOSE cells was observed for up to 10 $\mu\text{mol/L}$ concentration of HO-3867. However, treatment with 20 $\mu\text{mol/L}$ H-4073 or HO-3867 showed significant cytotoxicity to hOSE cells. Taken together, the cellular viability studies showed that both H-4073 and HO-3867 were comparably and significantly effective

in inducing cytotoxicity in A2780 and other ovarian cancer cell lines; however, HO-3867 was significantly less toxic to noncancerous hOSE cells when compared with H-4073.

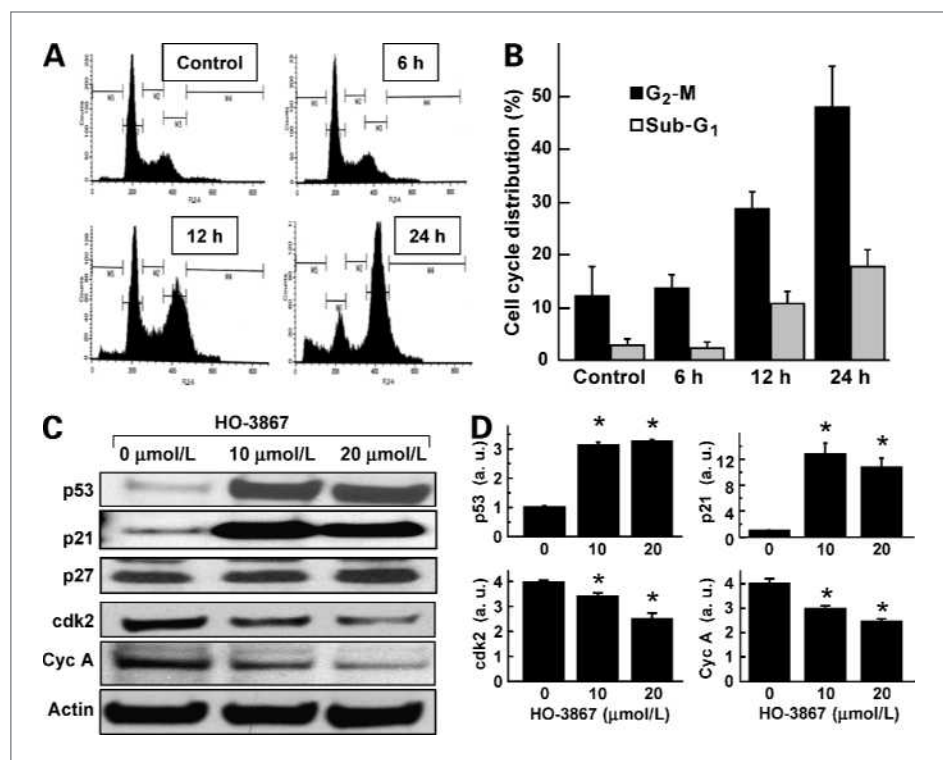
HO-3867 induces G₂-M cell cycle arrest in A2780 cells

We next examined whether the growth inhibition of A2780 cells by HO-3867 was caused by cell cycle arrest. Cells were treated with HO-3867 for 6, 12, or 24 hours; fixed; and cell cycle populations were determined by flow cytometry. The results showed that the percentages of the cell population in the G₂-M and sub-G₁ phases were significantly higher in the treatment group when compared with the nontreated control group (Fig. 2A and B). We then determined the effect of HO-3867 on the cell cycle regulatory molecules p53, p21, p27, cdk2, and cyclin A (Fig. 2C) by Western blotting. The levels of p53 and p21 were significantly upregulated, whereas cdk2 and cyclin-A levels were significantly decreased after treatment (Fig. 2D). These results indicated that HO-3867 caused G₂-M cell cycle arrest, at least in part, by modulating cell cycle regulatory proteins.

HO-3867 induces apoptosis in A2780 cells

The arrest of cell cycle progression in cancer cells is usually associated with the concomitant activation of proapoptotic pathways. To determine whether HO-3867-induced cell cycle arrest led to apoptosis, the expression of activated caspases were probed by Western blotting.

Figure 2. Modulation of cell cycle progression and cell cycle regulatory proteins by HO-3867. A2780 cells were treated with HO-3867 for 6, 12, or 24 hours. A, representative flow cytometry profiles of control (0 $\mu\text{mol/L}$) and HO-3867 (20 $\mu\text{mol/L}$) treatment groups at different time periods. B, quantitative cell cycle (DNA content) distribution (% of total) in the control and treatment groups. Columns, mean ($n = 5$); bars, SD; *, $P < 0.01$ versus control. C, immunoblot images of cell cycle regulatory proteins. D, quantitative results of p53, p21, cdk2, and cyclin A bands. Columns, mean ($n = 5$); bars, SD; *, $P < 0.01$ versus control (0 $\mu\text{mol/L}$); a.u., arbitrary units.



The blots showed the activation of caspase-8, caspase-7, cleaved caspase-3, and PARP in A2780 cells treated with HO-3867 for 24 hours (Fig. 3A). The quantitative results of the immunoblots (Fig. 3B) showed a significant increase in the level of these caspases in cells treated with HO-3867 when compared with nontreated cells. We further determined the levels of caspase-8-associated death receptors such as Fas/CD95 and Fas-L. The data from the Fas/CD95 expression showed a clear increase in HO-3867-treated cells when compared with nontreated group. However, no significant change was observed in Fas-L (data not shown).

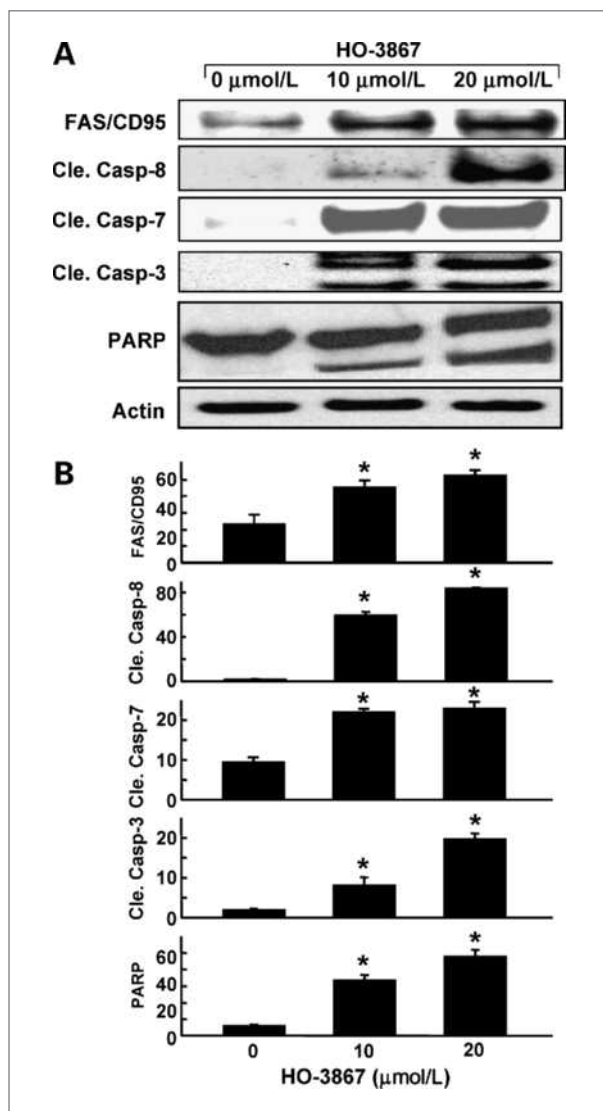


Figure 3. Induction of apoptosis by HO-3867. A2780 cells were treated with HO-3867 for 24 hours and subjected to Western blot analysis for apoptotic marker proteins. A, representative immunoblot images of FAS/CD95, cleaved caspases (cle. casp; 8, 7, and 3), and PARP. B, quantitative results of immunoblot. Columns, mean ($n = 5$) expressed as arbitrary units; bars, SD; *, $P < 0.01$ versus control (0 $\mu\text{mol/L}$).

HO-3867 inhibits the JAK/STAT3 pathway

The constitutive activation of STAT3 in ovarian cancer has been shown to regulate the expression of genes implicated in tumor-cell proliferation and survival (36, 37). To determine whether the HO-3867-induced growth inhibition in A2780 cell was mediated by STAT3, we examined the level of phosphorylated STAT3 (pSTAT3) by Western blotting (Fig. 4A). The pSTAT3 (Tyr705 and Ser727) levels were significantly decreased after treatment with 10 or 20 $\mu\text{mol/L}$ HO-3867 for 24 hours. Excessive JAK activity in tumor cells is one of the most common mechanisms for constitutive activation of STAT3. To examine whether HO-3867 exposure resulted in a decrease in STAT3 activation through JAK kinase inhibition, we measured the phosphorylated level of JAK1 after 24 hours of exposure to 10 or 20 $\mu\text{mol/L}$ HO-3867 (Fig. 4A). In addition, we cross-checked the expression of these proteins using immunoprecipitation and confirmed the decreased expression of pSTAT3 and pJAK1 with no change in the total expression levels of these proteins. The data showed a substantial decrease in phospho-JAK1 (Tyr1022/1023) when compared with unexposed controls, suggesting that HO-3867 blocked the JAK/STAT3 pathway. Before proceeding to *in vivo* experiments, we confirmed the potent apoptosis-inducing effect of HO-3867 in four additional ovarian cancer cell lines, A2780R, SKOV3, OV4, and OVCAR3. Following HO-3867 treatment, all four cell lines clearly showed caspase-3 and PARP cleavage, accompanied by a decrease in the expression levels of pSTAT3 and JAK1 (Fig. 4B). The results suggested that induction of apoptosis and inhibition of JAK/STAT3 signaling could be caused by HO-3867 in human ovarian cancer cell lines.

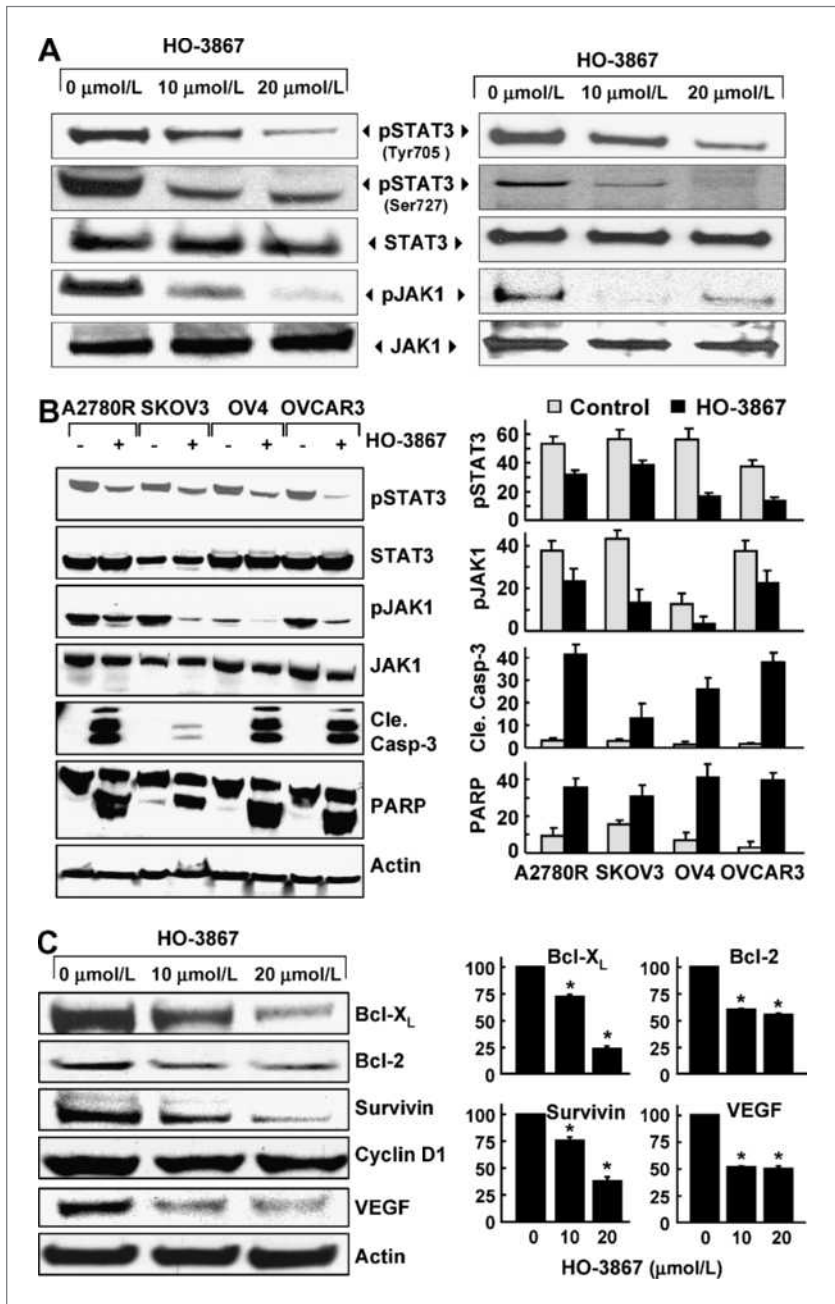
HO-3867 downregulates the STAT3 target proteins

To investigate the downstream consequences of STAT3 inhibition, Western blotting was done to determine the protein levels of Bcl-xL, Bcl-2, survivin, vascular endothelial growth factor (VEGF), and cyclin D1 following 24-hour exposure to HO-3867 at 10 and 20 $\mu\text{mol/L}$ concentrations. There was a clear reduction in Bcl-xL, Bcl-2, survivin, and VEGF levels, whereas no significant change in cyclin D1 level was observed (Fig. 4C). Because these proteins are involved in anti-apoptotic (survivin, Bcl-2, and Bcl-xL) and angiogenic (VEGF) protein expressions, the downregulation of these proteins suggested profound antitumor potential of HO-3867 in ovarian cancer cells. The results clearly showed the involvement of the STAT3 pathway in the growth inhibition of the A2780 ovarian cancer cells by HO-3867.

HO-3867 inhibits the growth of xenograft tumor in mice

Based on our *in vitro* results, which showed significant cytotoxicity of HO-3867 to human ovarian cancer cell lines, we next evaluated the efficacy of HO-3867 in a human ovarian tumor xenograft grown in the back of mice. The mice were treated with HO-3867 and the tumor size

Figure 4. Inhibition of JAK/STAT3-signaling and downstream proteins by HO-3867. Cells were treated with HO-3867 for 24 hours and subjected to Western blot analysis. A, representative immunoblot images of phosphorylated and total STAT3 and JAK1 in A2780 cells and immunoprecipitation results of pSTAT3 (Tyr705/Ser727) and pJAK1 (Tyr1022/1023) using bands captured by STAT3 or JAK1 and blotted with pSTAT3 or pJAK1. B, representative Western blots obtained from four other ovarian cancer cell lines (A2780R, SKOV3, OV4, and OVCAR3) treated with 10 $\mu\text{mol/L}$ HO-3867 for 24 hours. Note the decreased levels of pJAK1 and pSTAT3, and corresponding increased levels of cleaved caspase-3 and cleaved PARP in the treated cells compared with nontreated cells. Densitometric analysis of Western blots are shown for pJAK1, pSTAT3, cleaved caspase-3, and cleaved PARP. Columns, mean ($n = 5$) expressed as arbitrary units; bars, SD. C, immunoblot images of Bcl-xL, Bcl-2, survivin, cyclin D1, and VEGF proteins in cells. Quantitative results of Bcl-xL, Bcl-2, survivin, and VEGF bands are shown. Columns, mean ($n = 5$) expressed as a percent of control (*, $P < 0.01$); bars, SD.



was measured twice weekly for 5 weeks as reported (10, 15). A significant reduction in the tumor volume was observed in a dose-dependent manner; particularly, the doses of 50 and 100 ppm were more effective when compared with vehicle-treated controls (Fig. 5). We also measured the body weight and diet consumption of tumor-bearing animals. HO-3867-treated animals did not show any gross signs of toxicity and/or possible adverse side effects as measured by two profiles: body weight (Fig. 5C) and diet consumption (Fig. 5D). These results

suggest the *in vivo* antitumor efficacy of HO-3867 against ovarian tumor without any apparent signs of toxicity.

HO-3867 inhibits pSTAT3 and downregulates the STAT3-targeting proteins *in vivo*

We further analyzed the excised tumor tissue to determine whether HO-3867 inhibited the STAT3/JAK protein expression levels, as observed in the *in vitro* studies. In concert with the decreased expressions in both pSTAT3 Tyr705 and Ser727 levels, without affecting total STAT3,

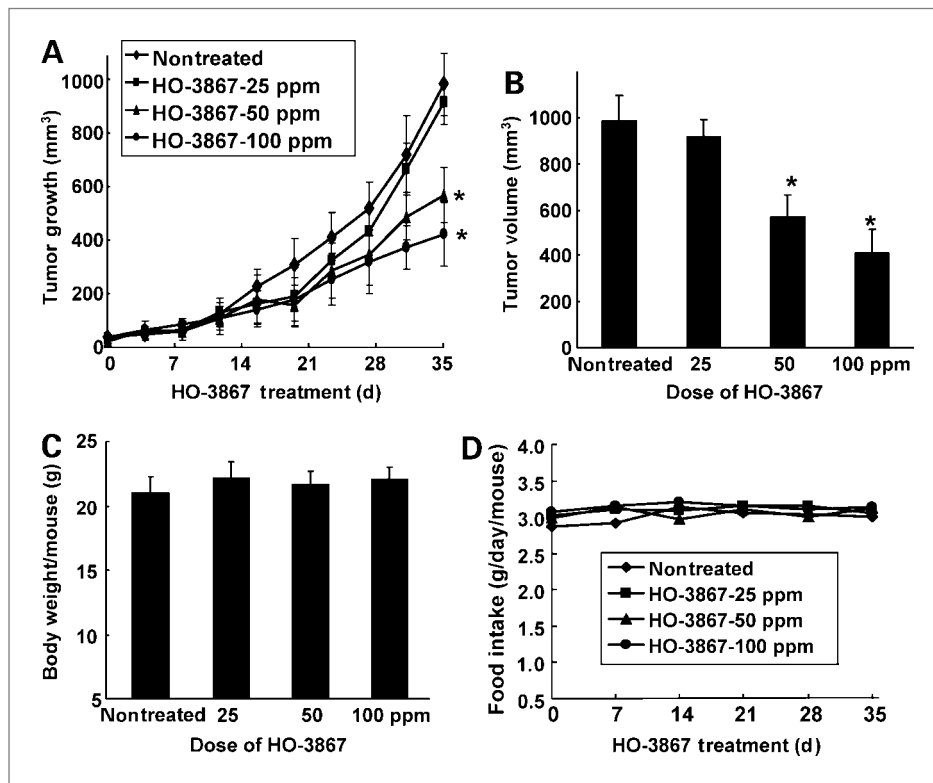


Figure 5. Effect of HO-3867 on murine xenograft tumors. A, a dose-dependent decrease in the volume of the xenograft tumors growth is observed following HO-3867 treatment. B, final volume of HO-3867-treated tumors at the 5th week. C, change in body weight and D, consumption of feed containing HO-3867 over time. Points, mean from nine mice in each group; bars, SEM. *, $P < 0.05$ versus nontreated control group.

we observed a clear downregulation of total JAK levels in tumor tissues. However, we did not observe any significant change in pJAK levels in tumor tissues (Fig. 6A). As for the target gene products of STAT3, we observed a clear decrease of cyclin D1, VEGF, Bcl-2, and Survivin levels in the HO-3867-treated tumors (Fig. 6B). Interestingly, we noticed a significant induction of cleaved caspase-3 and PARP, which is a known marker of apoptosis and a downstream target of activated caspase-3 (Fig. 6C and D; ref. 38), suggesting that HO-3867 induced apoptosis *in vivo*.

Discussion

The results of the present study established that the difluorodiarlylidene piperidone, HO-3867, exhibits potent anticancer efficacy toward human ovarian cancer cells and xenograft tumors. HO-3867, which also incorporates an antioxidant function, exhibits substantially lower toxicity toward noncancerous cells. The mechanistic studies revealed that HO-3867 targets multiple pathways, including altering the proteins involved in G₂-M cell cycle arrest, increased expression of Fas/CD95, downregulation of antiapoptotic signals, and inhibition of the JAK/STAT3 pathway in both *in vitro* and *in vivo*.

Cell cycle control plays a critical role in the regulation of tumor cell proliferation. Many cytotoxic agents arrest cell cycle at the G₁, S, or G₂-M phase. In the present study, HO-3867 induced G₂-M cell cycle arrest in A2780 cells as evidenced by a significant increase in the p53, p21, and

p27 protein levels. We also observed a significant reduction in Cdk2 and cyclin A levels. Previous studies have shown that the G₂-M-phase progression is regulated by a number of Cdk/cyclins as well as Cdk inhibitors such as p21 and p27 (23). Hence, our results suggest that the HO-3867-induced G₂-M cell cycle arrest is mediated by the induction of p53 and p21 and downregulation of cyclin A and Cdk2.

Many curcumin derivatives induce apoptosis in cancer cells, but the mechanisms by which they do so differ (22, 23). The death receptor-associated mechanism has been recently receiving much attention for the anticancer activity of curcumin derivatives (39, 40). We observed that the death receptor gene *Fas/CD95* was activated in A2780 cells by HO-3867. We further observed that the expression level of TNF-R1, the receptor of tumor necrosis factor- α , was unchanged in the HO-3867-treated A2780 cells (data not shown). It has been reported that curcumin promoted tumor necrosis factor- α -induced apoptosis in a variety of cancer cells, but without a significant increase in the TNF-R1 expression level. Curcumin and curcumin analogues have also been shown to upregulate death receptor 5 and FasL expression, thereby inducing apoptosis in human cancer cells (23, 41). Thus, our results suggest a critical involvement of upregulated death receptor superfamily-mediated signals in the stimulation of A2780 apoptosis following HO-3867 exposure.

STAT3 has been shown to suppress the transcription of *Fas/CD95* (42). This suggests the HO-3867-mediated

downregulation of STAT3 expression, in both *in vitro* and *in vivo*, as a putative mechanism for increased Fas/CD95 expression. This is obvious from the substantial decrease in the level of Tyr705-pSTAT3, a major active form of activated STAT3. It is noteworthy that the expression level of Ser727-pSTAT3 was also clearly decreased *in vivo*. Because the Ser727 phosphorylation is also known to regulate the transcriptional activity of STAT3 (20, 21), this attenuated phosphorylation is suggested to participate in the downregulation of the transcriptional activity of STAT3 in the xenograft tumor treated with HO-3867. We also observed that HO-3867 caused a substantial inhibition of phospho-JAK1 (Tyr-1022/1023), suggesting that HO-3867 can inhibit the constitutive activation of STAT3, which may be caused, at least in part, by the inhibition of pJAK1. However, HO-3867 may also inhibit STAT3 activation through JAK2, Src, Erb2, and epidermal growth factor receptor, which are implicated in STAT3 activation as well. Additional studies are needed to explore these pathways.

Downstream proteins of STAT3 have been shown to regulate apoptosis and regulation in cancer cells. For example, Bcl-xL, Bcl-2, and survivin have been shown to suppress apoptosis, whereas *c-myc* and cyclin D1 have been shown to mediate proliferation (43, 44). Because of the fact that STAT3-downregulating genes are all critically involved in the development of cancer aggressiveness, targeting STAT3 is considered a potential anticancer strategy. Furthermore, inhibition of STAT3 expression *in vivo* has provided deep insight into a new approach for the treatment of human tumors (16, 45). In addition, inhibi-

tion of STAT3 activation is valid in inducing significant apoptosis in both the mice model of melanoma xenografts and that of squamous cell carcinoma xenografts (8). The induction of apoptosis in tumor is another approach to limit their uncontrolled proliferation of tumor growth. In this process, activation of caspases is the central event (46). Once activated, the executioner caspases downstream of the cascade act on the key molecules inside the cells to orchestrate cell death. In the present study, we observed that HO-3867 clearly induces apoptotic death both *in vitro* and *in vivo*, at least in part, due to the activation of caspase-3 and cleavages of PARP. Cleavage of PARP by activated caspases is considered as a marker for apoptotic death (38). STAT3 is also known to protect cells from apoptosis through the upregulation of Bcl-xL, Bcl-2, and survivin (15). The expression levels in all of these molecules downstream of STAT3 activation were clearly reduced in ovarian cancer cells by exposure to HO-3867, not only *in vitro* but also *in vivo*—even in mice given a low concentration (50 ppm) of HO-3867. This implies that induction of apoptosis may be an additional contributing factor in the HO-3867-mediated inhibition of ovarian tumor growth. However, further studies are essential to elucidate the mechanism of apoptosis induction by HO-3867.

In summary, we have investigated the anticancer efficacy of a novel curcuminoid compound, HO-3867, which inhibited ovarian tumor growth by inhibition of the JAK1/STAT3 signaling pathway. HO-3867 shows substantial promise for further development as a potential agent for treating ovarian cancer.

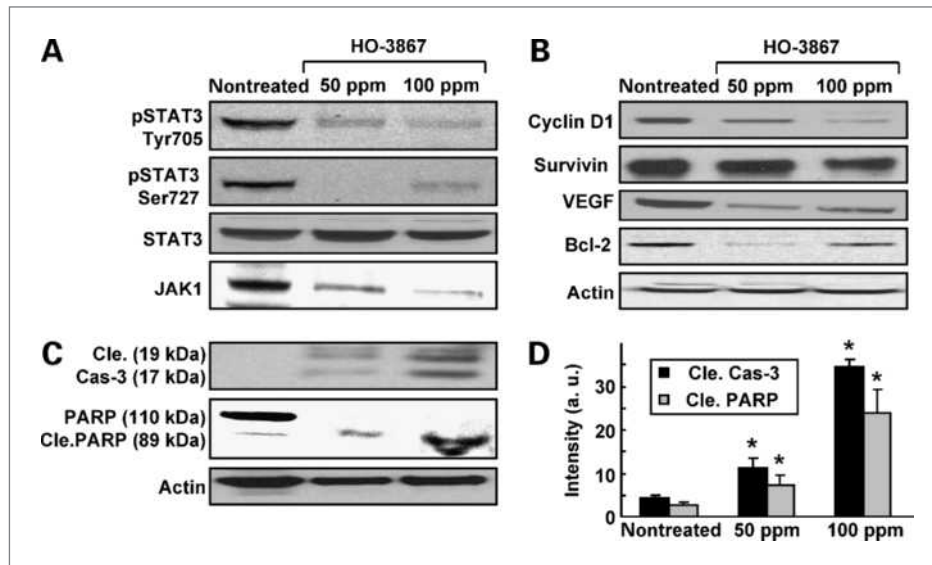


Figure 6. Effect of HO-3867 on the expression of JAK/STAT3 and targeting genes. A, immunoblot analysis using tissue lysates of xenograft tumors. The decreased expression of pSTAT3 Tyr705 and Ser727 and JAK1 are noted in the HO-3867-treated tumor lysates in a dose-dependent manner in concert with decreased expression of both Tyr705-phosphorylated and Ser727-pSTAT3. B, the decreased expression is also shown in cyclin D1, Bcl-2, and VEGF in a dose-dependent manner. C, cleavage of caspase-3 and PARP in HO-3867-treated tumor lysates in a dose-dependent manner. D, quantification of cleaved caspase-3 and cleaved PARP. *, $P < 0.05$ versus respective untreated control group.

Disclosure of Potential Conflicts of Interest

No potential conflicts of interest were disclosed.

Acknowledgments

We thank Mária Balog for her help with the synthesis of the compounds.

Grant Support

NIH grant CA102264 (P. Kuppusamy), The Kaleidoscope of Hope Foundation grant (K. Selvendiran), and Hungarian Research Fund Grant OTKA K81123 (K. Hideg).

The costs of publication of this article were defrayed in part by the payment of page charges. This article must therefore be hereby marked *advertisement* in accordance with 18 U.S.C. Section 1734 solely to indicate this fact.

Received 12/28/2009; revised 02/12/2010; accepted 02/26/2010; published OnlineFirst 05/04/2010.

References

- Jemal A, Siegel R, Ward E, et al. Cancer statistics, 2008. *CA Cancer J Clin* 2008;58:71–96.
- Ozols RF, Bookman MA, Connolly DC, et al. Focus on epithelial ovarian cancer. *Cancer Cell* 2004;5:19–24.
- Bristow RE, Chi DS. Platinum-based neoadjuvant chemotherapy and interval surgical cytoreduction for advanced ovarian cancer: a meta-analysis. *Gynecol Oncol* 2006;103:1070–6.
- Harries M, Gore M. Part II: chemotherapy for epithelial ovarian cancer-treatment of recurrent disease. *Lancet Oncol* 2002;3:537–45.
- Harries M, Gore M. Part I: chemotherapy for epithelial ovarian cancer-treatment at first diagnosis. *Lancet Oncol* 2002;3:529–36.
- Borst P, Rottenberg S, Jonkers J. How do real tumors become resistant to cisplatin? *Cell Cycle* 2008;7:1353–9.
- Raj MH, Abd Elmaged ZY, Zhou J, et al. Synergistic action of dietary phyto-antioxidants on survival and proliferation of ovarian cancer cells. *Gynecol Oncol* 2008;110:432–8.
- Yu H, Jove R. The STATs of cancer-new molecular targets come of age. *Nat Rev Cancer* 2004;4:97–105.
- Lu Y, Zhou J, Xu C, et al. JAK/STAT and PI3K/AKT pathways form a mutual transactivation loop and afford resistance to oxidative stress-induced apoptosis in cardiomyocytes. *Cell Physiol Biochem* 2008;21:305–14.
- Selvendiran K, Bratasz A, Tong L, Ignarro LJ, Kuppusamy P. NCX-4016, a nitro-derivative of aspirin, inhibits EGFR and STAT3 signaling and modulates Bcl-2 proteins in cisplatin-resistant human ovarian cancer cells and xenografts. *Cell Cycle* 2008;7:81–8.
- Yang F, Van Meter TE, Buettner R, et al. Sorafenib inhibits signal transducer and activator of transcription 3 signaling associated with growth arrest and apoptosis of medulloblastomas. *Mol Cancer Ther* 2008;7:3519–26.
- Clevenger CV. Roles and regulation of stat family transcription factors in human breast cancer. *Am J Pathol* 2004;165:1449–60.
- Durrant D, Richards JE, Walker WT, Baker KA, Simoni D, Lee RM. Mechanism of cell death induced by *cis*-3, 4', 5-trimethoxy-3'-aminostilbene in ovarian cancer. *Gynecol Oncol* 2008;110:110–7.
- Trachootham D, Zhou Y, Zhang H, et al. Selective killing of oncogenically transformed cells through a ROS-mediated mechanism by β -phenylethyl isothiocyanate. *Cancer Cell* 2006;10:241–52.
- Selvendiran K, Koga H, Ueno T, et al. Luteolin promotes degradation in signal transducer and activator of transcription 3 in human hepatoma cells: an implication for the antitumor potential of flavonoids. *Cancer Res* 2006;66:4826–34.
- Bharti AC, Shishodia S, Reuben JM, et al. Nuclear factor- κ B and STAT3 are constitutively active in CD138+ cells derived from multiple myeloma patients, and suppression of these transcription factors leads to apoptosis. *Blood* 2004;103:3175–84.
- Kim HY, Park EJ, Joe EH, Jou I. Curcumin suppresses Janus kinase-STAT inflammatory signaling through activation of Src homology 2 domain-containing tyrosine phosphatase 2 in brain microglia. *J Immunol* 2003;171:6072–9.
- Weir NM, Selvendiran K, Kutala VK, et al. Curcumin induces G₂/M arrest and apoptosis in cisplatin-resistant human ovarian cancer cells by modulating Akt and p38 MAPK. *Cancer Biol Ther* 2007;6:178–84.
- Lin YG, Kunnumakkara AB, Nair A, et al. Curcumin inhibits tumor growth and angiogenesis in ovarian carcinoma by targeting the nuclear factor- κ B pathway. *Clin Cancer Res* 2007;13:3423–30.
- Adams BK, Ferstl EM, Davis MC, et al. Synthesis and biological evaluation of novel curcumin analogs as anti-cancer and anti-angiogenesis agents. *Bioorg Med Chem* 2004;12:3871–83.
- Adams BK, Cai J, Armstrong J, et al. EF24, a novel synthetic curcumin analog, induces apoptosis in cancer cells via a redox-dependent mechanism. *Anticancer Drugs* 2005;16:263–75.
- Subramaniam D, May R, Sureban SM, et al. Diphenyl difluoroketone: a curcumin derivative with potent *in vivo* anticancer activity. *Cancer Res* 2008;68:1962–9.
- Selvendiran K, Tong L, Vishwanath S, et al. EF24 induces G₂/M arrest and apoptosis in cisplatin-resistant human ovarian cancer cells by increasing PTEN expression. *J Biol Chem* 2007;282:28609–18.
- Tazi MF, Selvendiran K, Kuppusamy ML, et al. Evaluation of a novel class of fluorinated curcumin analogs for safe and targeted anticancer therapy (STAT). *Free Radic Biol Med* 2008;45:S56–7.
- Selvendiran K, Ahmed S, Dayton A, et al. Safe and targeted anticancer efficacy of a novel class of antioxidantconjugated difluorodiarlylidene-piperidones: differential cytotoxicity in healthy and cancer cells. *Free Radic Biol Med* 2010;48:1228–35.
- Injac R, Strukelj B. Recent advances in protection against doxorubicin-induced toxicity. *Technol Cancer Res Treat* 2008;7:497–516.
- Santos NA, Bezerra CS, Martins NM, Curti C, Bianchi ML, Santos AC. Hydroxyl radical scavenger ameliorates cisplatin-induced nephrotoxicity by preventing oxidative stress, redox state imbalance, impairment of energetic metabolism and apoptosis in rat kidney mitochondria. *Cancer Chemother Pharmacol* 2008;61:145–55.
- Maliakel DM, Kagiya TV, Nair CK. Prevention of cisplatin-induced nephrotoxicity by glucosides of ascorbic acid and α -tocopherol. *Exp Toxicol Pathol* 2008;60:521–7.
- Conklin KA. Dietary antioxidants during cancer chemotherapy: impact on chemotherapeutic effectiveness and development of side effects. *Nutr Cancer* 2000;37:1–18.
- Samuni Y, Gamsan J, Samuni A, et al. Factors influencing nitroxide reduction and cytotoxicity *in vitro*. *Antioxid Redox Signal* 2004;6:587–95.
- Mitchell JB, Krishna MC, Kuppusamy P, Cook JA, Russo A. Protection against oxidative stress by nitroxides. *Exp Biol Med (Maywood)* 2001;226:620–1.
- Kuppusamy P, Li H, Ilangovan G, et al. Noninvasive imaging of tumor redox status and its modification by tissue glutathione levels. *Cancer Res* 2002;62:307–12.
- Kuppusamy P, Wang P, Shankar RA, et al. *In vivo* topical EPR spectroscopy and imaging of nitroxide free radicals and polynitroxyl-albumin. *Magn Reson Med* 1998;40:806–11.
- Hankovzky HO, Hideg K, Lex L. Nitroxyls VII. synthesis and reactions of highly reactive 1-oxyl-2,2,5,5-tetramethyl-2,5-dihydropyrrole-3-ylmethyl sulfonates. *Synthesis* 1980:914–6.
- Kalai T, Tong L, Balog M, Selvendiran K, Kuppusamy P, Hideg K. Synthesis of N-substituted 3,5-bis(arylidene)-4-piperidones with high antitumor and antioxidant activity. *Bioorg Med Chem* 2010, in preparation.
- Bromberg JF, Wrzeszczynska MH, Devgan G, et al. Stat3 as an oncogene. *Cell* 1999;98:295–303.

37. Burke WM, Jin X, Lin HJ, et al. Inhibition of constitutively active Stat3 suppresses growth of human ovarian and breast cancer cells. *Oncogene* 2001;20:7925–34.
38. Duriez PJ, Shah GM. Cleavage of poly(ADP-ribose) polymerase: a sensitive parameter to study cell death. *Biochem Cell Biol* 1997;75:337–49.
39. Deeb D, Jiang H, Gao X, et al. Curcumin [1,7-bis(4-hydroxy-3-methoxyphenyl)-1–6-heptadine-3,5-dione; C₂₁H₂₀O₆] sensitizes human prostate cancer cells to tumor necrosis factor-related apoptosis-inducing ligand/Apo2L-induced apoptosis by suppressing nuclear factor-κB via inhibition of the prosurvival Akt signaling pathway. *J Pharmacol Exp Ther* 2007;321:616–25.
40. Gadducci A, Cosio S, Muraca S, Genazzani AR. Molecular mechanisms of apoptosis and chemosensitivity to platinum and paclitaxel in ovarian cancer: biological data and clinical implications. *Eur J Gynaecol Oncol* 2002;23:390–6.
41. Jung EM, Park JW, Choi KS, et al. Curcumin sensitizes tumor necrosis factor-related apoptosis-inducing ligand (TRAIL)-mediated apoptosis through CHOP-independent DR5 upregulation. *Carcinogenesis* 2006;27:2008–17.
42. Ivanov VN, Bhoumik A, Krasilnikov M, et al. Cooperation between STAT3 and c-jun suppresses Fas transcription. *Mol Cell* 2001;7:517–28.
43. Kim KW, Mutter RW, Cao C, et al. Inhibition of signal transducer and activator of transcription 3 activity results in down-regulation of Survivin following irradiation. *Mol Cancer Ther* 2006;5:2659–65.
44. Nielsen M, Kaestel CG, Eriksen KW, et al. Inhibition of constitutively activated Stat3 correlates with altered Bcl-2/Bax expression and induction of apoptosis in mycosis fungoides tumor cells. *Leukemia* 1999;13:735–8.
45. Metz S, Naeth G, Heinrich PC, Muller-Newen G. Novel inhibitors for murine and human leukemia inhibitory factor based on fused soluble receptors. *J Biol Chem* 2008;283:5985–95.
46. Ziegler DS, Kung AL. Therapeutic targeting of apoptosis pathways in cancer. *Curr Opin Oncol* 2008;20:97–103.

Molecular Cancer Therapeutics



Anticancer Efficacy of a Difluorodiarylidanyl Piperidone (HO-3867) in Human Ovarian Cancer Cells and Tumor Xenografts

Karuppaiyah Selvendiran, Liyue Tong, Anna Bratasz, et al.

Mol Cancer Ther 2010;9:1169-1179. Published OnlineFirst May 4, 2010.

Updated version Access the most recent version of this article at:
doi:[10.1158/1535-7163.MCT-09-1207](https://doi.org/10.1158/1535-7163.MCT-09-1207)

Cited Articles This article cites by 44 articles, 14 of which you can access for free at:
<http://mct.aacrjournals.org/content/9/5/1169.full.html#ref-list-1>

Citing articles This article has been cited by 4 HighWire-hosted articles. Access the articles at:
<http://mct.aacrjournals.org/content/9/5/1169.full.html#related-urls>

E-mail alerts [Sign up to receive free email-alerts](#) related to this article or journal.

Reprints and Subscriptions To order reprints of this article or to subscribe to the journal, contact the AACR Publications Department at pubs@aacr.org.

Permissions To request permission to re-use all or part of this article, contact the AACR Publications Department at permissions@aacr.org.